

# Bright X-ray flares in XRF 050406 and GRB 050502B provide evidence for extended central engine activity

D. N. Burrows<sup>1</sup>, P. Romano<sup>2</sup>, A. Falcone<sup>1</sup>, S. Kobayashi<sup>1,3</sup>, B. Zhang<sup>4</sup>, A. Moretti<sup>2</sup>,  
P. T. O'Brien<sup>5</sup>, M. R. Goad<sup>5</sup>, S. Campana<sup>2</sup>, K. L. Page<sup>5</sup>, L. Angelini<sup>6,7</sup>, S. Barthelmy<sup>6</sup>,  
A. P. Beardmore<sup>5</sup>, M. Capalbi<sup>8</sup>, G. Chincarini<sup>2,9</sup>, J. Cummings<sup>6</sup>, G. Cusumano<sup>10</sup>,  
D. Fox<sup>11</sup>, P. Giommi<sup>8</sup>, J. E. Hill<sup>1</sup>, J. A. Kennea<sup>1</sup>, H. Krimm<sup>6</sup>, V. Mangano<sup>10</sup>, F. Marshall<sup>6</sup>,  
P. Mészáros<sup>1</sup>, D. C. Morris<sup>1</sup>, J. A. Nousek<sup>1</sup>, J. P. Osborne<sup>5</sup>, C. Pagani<sup>1,2</sup>, M. Perri<sup>8</sup>,  
G. Tagliaferri<sup>2</sup>, A. A. Wells<sup>5</sup>, S. Woosley<sup>12</sup>, N. Gehrels<sup>6</sup>

---

<sup>1</sup> Department of Astronomy & Astrophysics, Pennsylvania State University, 525 Davey Lab, University Park, PA, 16802, USA

<sup>2</sup> INAF-Osservatorio Astronomico di Brera, Via Bianchi 46, 23807 Merate, Italy

<sup>3</sup> Center for Gravitational Wave Physics, Pennsylvania State University, 104 Davey Lab, University Park, PA, 16802, USA

<sup>4</sup> Department of Physics, University of Nevada, Box 454002, Las Vegas, NV, 89154-4002, USA

<sup>5</sup> Department of Physics and Astronomy, University of Leicester, University Road, Leicester LE1 7RH, UK

<sup>6</sup> NASA/Goddard Space Flight Center, Greenbelt, MD, 20771, USA

<sup>7</sup> Department of Physics and Astronomy, Johns Hopkins University, 3400 North Charles Street, Baltimore, MD, 21218, USA

<sup>8</sup> ASI Science Data Center, Via Galileo Galilei, 00044 Frascati, Italy

<sup>9</sup> Dipartimento di Fisica, Università degli studi di Milano-Bicocca, Piazza delle Scienze 3, 20126, Milan, Italy

<sup>10</sup> INAF- Istituto di Astrofisica Spaziale e Fisica Cosmica Sezione di Palermo, Via Ugo La Malfa 153, 90146 Palermo, Italy

<sup>11</sup> Department of Astronomy, California Institute of Technology, MS 105-24, Pasadena, CA, 91125, USA

<sup>12</sup> Department of Astronomy & Astrophysics, University of California, Santa Cruz, CA, 95064, USA

**Gamma-ray bursts (GRBs) are the most powerful explosions since the Big Bang, with typical energies around  $10^{51}$  ergs. Long GRBs (duration  $> 2$  s) are thought to signal the creation of black holes, most likely by collapse of massive stars<sup>1,2,3</sup>. The detected signals from the resulting highly relativistic fireball consist of prompt gamma-ray emission (from internal shocks in the fireball) lasting for several seconds to minutes, followed by afterglow emission (from external shocks as the fireball encounters surrounding material) covering a broad range of frequencies from radio through X-rays<sup>4,5,6</sup>. Because of the time needed to determine the GRB position, most afterglow measurements have been made hours after the burst, and little is known about the characteristics of afterglows in the minutes following a burst, when the afterglow emission is actively responding to inhomogeneities in both the fireball and the circumburst environment. Here we report our discovery of two bright X-ray flares peaking a few minutes after the burst. These amazingly strong, rapid X-ray flares imply that the central engines of the bursts are active at much later times than previously thought, with strong internal shocks continuing for hundreds of seconds after the gamma-ray emission has ended.**

The *Swift*<sup>7</sup> X-ray Telescope (XRT)<sup>8</sup> provides unique and novel X-ray observations of young gamma-ray burst (GRB) afterglows, beginning in the first few minutes after the burst. (Here we use the terms “burst” and “prompt emission” to refer to the burst seen in hard X-rays and gamma rays, and the term “afterglow” to refer to the soft X-ray and optical emission seen after the end of the detectable hard X-ray prompt emission.) Between 23 December 2004 and 5 May 2005, the XRT observed 13 afterglows within 200 seconds of the burst for GRBs discovered by the *Swift* Burst Alert Telescope (BAT)<sup>9</sup>. In most cases the XRT found a monotonically decaying afterglow<sup>10,11,12,13</sup>. However,

there are a few notable exceptions. The afterglows of both XRF 050406 and GRB 050502B (see Table 1 for burst properties) were a factor of 10 – 1000 times fainter than previous XRT-detected afterglows at T+100 s, but brightened rapidly several minutes later before decaying back to their pre-flare fluxes (Figure 1). The afterglow of XRF 050406 brightens by a factor of 6 between 150 and 213 s post-burst. GRB 050502B has an even stronger flare, brightening by a factor of  $\sim$ 300 to a peak at T+740 s. Early X-ray flares similar to XRF 050406 have been seen occasionally in much brighter bursts<sup>14</sup>, but there are no previous observations of a giant X-ray flare like that seen in GRB 050502B.

The rise and fall of the flare in XRF 050406 are both very steep. When fit with power-law slopes using the burst trigger as the reference time, we find  $\alpha = +4.9 \pm 0.3$  during the rising portion, and  $\alpha = -5.7 \pm 0.6$  during the decay, with  $\delta t/t_{peak} \sim 0.3$  and 0.6 for the rise and fall times, respectively. (The flare slopes are more symmetrical when the underlying afterglow decay is subtracted off.) Such large slopes cannot be explained by external forward shocks, where the radiation physics implies a slow rise and decay, with the decay time  $\delta t$  comparable to the post-shock time  $t$  (ref. 15). The shape of the flare is reminiscent of an external reverse shock, but these are expected to be far less steep and should be seen in the optical, not the X-ray, band. Synchrotron self-Compton (SSC) models may be able to produce X-ray emission from a reverse shock, but only for carefully balanced conditions<sup>16</sup>. A far more natural explanation for this flare is continuation of strong internal shocks to a time of T+213 s.

The flare in GRB 050502B is slower, with  $\delta t_{decay}/t \sim 1$ , but the sharp spike at T+740 s (seen in the hard band in Figure 2b) argues against an external shock mechanism<sup>15</sup>. If produced by internal shocks, energy production by the central engine must continue for up to at least 740 s after the burst begins in this case.

Extended activity in the central engine can explain both of these flares. The central engine becomes active again around 150 seconds and 300 seconds after the burst for XRF 050406 and GRB 050502B, respectively. The duration of the rising portion of the flare directly measures the duration of the central engine activity because the observed time sequence essentially follows the central engine time sequence<sup>17</sup>. In this case, the late shocks that produce the flare must produce lower energy photons than the earlier internal shocks; this can be explained by smaller differences in relativistic Lorentz factor between shells in the fireball, combined with lower magnetic fields at the larger radius reached by the internal shocks at these late times. The flares have a total energy input comparable to or somewhat smaller than the prompt emission for both bursts. For the internal shock model, the typical peak energy is<sup>18</sup>  $E_p \propto L^{1/2} R^{-1} \propto L^{1/2} \Gamma^{-2} \delta t^{-1}$ , where  $L$  is the luminosity at the flare epoch,  $R$  is the internal shock distance,  $\Gamma$  is the Lorentz factor, and  $\delta t$  is the variability time-scale. For a radius  $R$  that is 3-10 times larger for the flare than the typical internal shock radius of the burst,  $E_p$  may be 10 times lower. This is consistent with the detection of these flares in the X-ray band rather than in gamma-rays, and with the large  $\delta t$  observed in the X-ray flares.

With the exception of the flare at 213s, the count rate of XRF 050406 was very low and detailed time-resolved spectroscopy is not possible. We can obtain some information on the spectral evolution of the flare, however, by dividing the data into two energy bands and examining light curves in those bands. Figure 2a shows the light curves in the 0.2-0.7 keV and 0.7-10 keV bands, together with the ratio of these bands. There is significant spectral evolution during the first 400 seconds of this afterglow. During the rising flare (about T+180s to T+200s) the hard band flux spikes up rapidly while the soft band flux remains constant, indicating that the flare is harder spectrally than the underlying afterglow. In fact, the rising portion of the flare contributes no significant flux between 0.2 and 0.7 keV, while increasing the count rate in the 0.7-10 keV band by a

factor of four. This provides strong constraints on the flare mechanism: it is difficult to quadruple the flux in the high energy band while the low energy band remains constant, unless the flare is strongly absorbed (by  $N_H \sim 10^{21} \text{ cm}^{-2}$ ). However, the soft band peaks during the time bin following the overall peak, indicating that the emission softens as the flare decays away. If absorption is invoked for the rising portion of the flare, then the absorption seems to decrease significantly during the flare decay, suggesting that the absorbing gas is being ionized by the flare. Following the flare the band ratio returns to a value consistent with the pre-flare values.

A band ratio plot of GRB 050502B also shows clear indications of spectral variations (Figure 2b), with a trend similar to that in XRF 050406 (hardening at the beginning of the flare and gradually softening as the flare progresses). However, the giant flare in GRB 050502B is bright enough to allow time-resolved spectroscopy during this flare. The spectral fits suggest that the photon index does not change during the flare, and the softening of the spectrum during the flare is caused by changes in the absorbing column. At the beginning of the flare, the spectrum indicates an excess absorbing column (in addition to the Galactic column in this direction, assuming redshift of zero) of  $(1.3 \pm 0.2) \times 10^{21} \text{ cm}^{-2}$ . This monotonically decreases to zero by the end of the flare (Figure 3).

The decreasing  $N_H$  provides direct evidence that the absorbing gas is being ionized during the flare, possibly by UV photons associated with the X-ray flare. The prompt UV emission associated with the burst may have been strongly suppressed by synchrotron self-absorption due to the small internal shock radius, leaving significant amounts of neutral gas along the line of sight, but this mechanism is not applicable to the flare, which occurs at a much larger radius. The UV flash associated with this flare can penetrate through the ISM for a long distance<sup>19</sup> (e.g.  $10^{19}$ - $10^{20} \text{ cm}$ ). Given a moderately dense ISM

( $n \sim 10 \text{ cm}^{-3}$ ), one can explain the ionization of the observed column densities of  $\sim 10^{21} \text{ cm}^{-2}$  in addition to the lack of detection of these flares by the *Swift* UVOT.

We have referred to these events as X-ray flares because they were not detected by the higher-energy BAT instrument on *Swift*. This is presumably due to the higher sensitivity of the XRT and to the steep photon index ( $\Gamma=2.3$  for XRF 050406 and  $\Gamma=2.4$  for GRB 050502B) of the afterglows. In the case of XRF 050406, the prompt emission was classified as an X-ray Flash due to its relatively soft spectrum. The discovery of these large X-ray flares in the afterglows raises the possibility that these flares themselves would be classified as X-ray Flashes, had they not been preceded by the brighter, and possibly higher-energy, bursts detected by the BAT. If a normal, relatively hard burst such as GRB 050502B can produce an X-ray flare through late-time internal shocks, this suggests that XRFs themselves may be related to the characteristics of the central engine rather than to geometrical effects<sup>20,21</sup>. However, the smooth temporal variations observed in these X-ray flares are somewhat different from those detected in XRFs<sup>27</sup>.

Both of these afterglows appear to be dominated by long periods of energy production by the central engine, leading to a long period of prompt emission from internal shocks. In addition to the large flares several minutes after the burst, the plateaus or bumps beginning several hours later imply that significant energy is being injected into the blast wave by refreshed shocks, or that the internal shocks are still continuing up to several days after the burst in the observer's frame. This implies that the central engine operated for a time much longer than the duration of the prompt emission recorded by the BAT. A possible mechanism for this activity is fallback of material into the central black hole, which could last for several days<sup>22</sup>. If the central engine is still pumping significant energy into the blast wave at such late times, how can one explain the short duration of the gamma-ray emission? It is possible that the same mechanism (perhaps low input

energies, low Lorentz factors or entrained baryons) that produces the low energies in the initial burst of XRF 050406 results in even lower energies at later times, pushing the late-time internal shock emission below the BAT energy band (15-150 keV). A similar mechanism may be operating in 050502B, though starting from a more energetic phase of prompt emission. The detailed study of these flares enabled by prompt *Swift* XRT observations will continue to shed light on these mechanisms as additional bright flares are discovered over the coming months and years.

**Acknowledgements** This letter is based on observations with the NASA Swift gamma-ray burst explorer. We thank the Swift operations team for their support. The authors acknowledge support from NASA, ASI, and PPARC.

**Competing Interests Statement** The authors declare that they have no competing financial interest.

**Correspondence** and requests for materials should be addressed to D. N. Burrows (email: [burrows@astro.psu.edu](mailto:burrows@astro.psu.edu)).

---

**Table 1 Burst Properties**

Burst Name	Trigger time	$T_{90}$ (s) <sup>†</sup>	Photon Index	Fluence (ergs cm <sup>-2</sup> )	Ref.
XRF 050406	6 April 2005 15:58:48 UTC	$5 \pm 1$	$2.4 \pm 0.3$	$9 \times 10^{-8}$	23, 24
GRB 050502B	2 May 2005 09:25:40 UTC	$17.5 \pm 0.2$	$1.6 \pm 0.1$	$8 \times 10^{-7}$	25, 26

---

<sup>†</sup>  $T_{90}$  is the burst duration, defined as the time within which 90% of the photons arrived.

XRF 050406 was discovered by the *Swift* BAT instrument at 15:58:48 UTC on 6 April 2005. It had a very soft spectrum (power-law spectrum  $N(E) \propto E^{-\Gamma}$  with photon index  $\Gamma=2.4$ ) and is classified as an X-ray Flash (XRF)<sup>27</sup>. The *Swift* observatory performed a prompt slew to the burst location, pointing the XRT and the UV-Optical Telescope (UVOT) toward the burst in  $\sim$ 84 seconds and the XRT executed its normal sequence of readout modes<sup>28</sup>. No bright source was found in the first 2.5 s XRT exposure, but the count rate began climbing rapidly about 180 s after the BAT trigger (Figure 1a). GRB 050502B was a typical multi-peaked burst discovered by the *Swift* BAT instrument at 09:25:40 UTC on 2 May 2005. The *Swift* observatory performed a prompt slew and the XRT began collecting data  $\sim$ 63 seconds after the burst trigger. No bright source was found in the first 2.5 s exposure. About 300 seconds after the burst, the X-ray intensity began to rise steeply, switching the XRT from Photon Counting (PC) mode into Windowed Timing (WT) mode through the peak at 740 s post-burst (Figure 1b; see ref. 28 for a discussion of XRT readout modes).

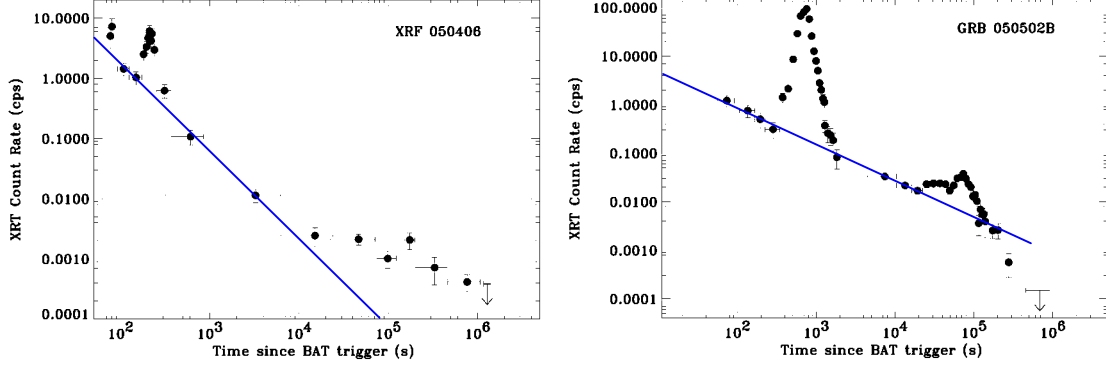


**Figure 1** Background-subtracted X-ray light curves of the afterglows of XRF 050406 (a) and GRB 050502B (b). The XRT data were processed using the `xrtpipeline` tool (Build 14) within the FTOOLS v6.0 software package. We applied standard screening to the data and included data between 0.2 and 10 keV. For XRF 050406 we obtained a total exposure time of 155 ks distributed over 17 days; for GRB 050502B the total exposure time was 176 ks seconds over 11 days. The light curves use WT mode data when the count rate is above about  $0.5 \text{ s}^{-1}$  (to avoid pile-up) and PC mode for lower count rates. The solid lines represent power-law fits to the underlying afterglow decays from about 100 s to 10,000 s ( $\alpha = -1.5 \pm 0.1$  and  $-0.8 \pm 0.2$  for XRF 050406 and GRB 050502B, respectively, where the X-ray flux varies as  $F_{\text{X}} \propto t^{\alpha}$ ). The bright X-ray flares are superposed on this underlying power-law decay. At later times the XRF 050406 light curve flattens, while the GRB 050502B has several bumps, both suggesting late-time energy injection into the external shock or continued internal shock activity. The rapid decline in count rate for GRB 050502B at  $T > 10^5 \text{ s}$  indicates a possible jet break at around 1-2 days post-burst. The last data point for GRB 050502B is a 95% confidence upper limit based on 82 ks of exposure time (nearly half the total).

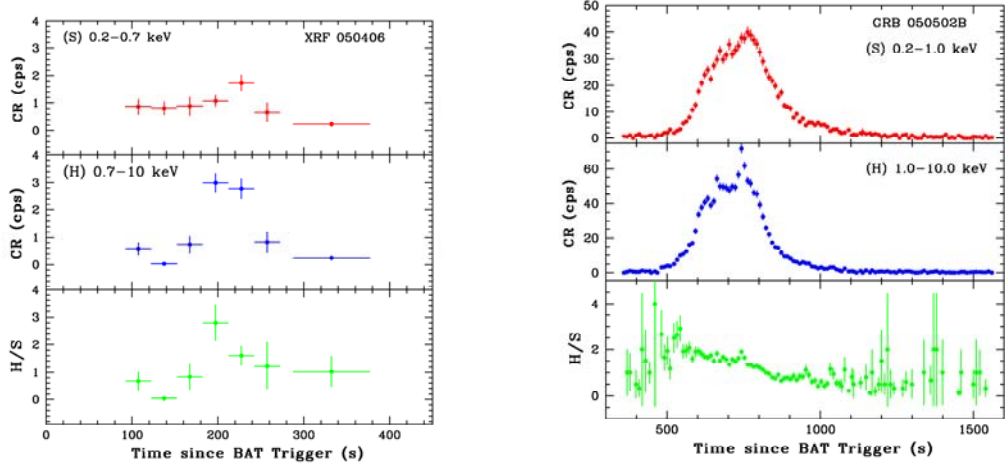


**Figure 2** Band ratio plots, showing spectral variations during the flares. In both cases the top two panels show the count rates in the soft and hard bands, while the bottom panel shows the band ratio (hard/soft). The boundaries between the hard and soft bands were chosen independently for each burst to provide comparable numbers of counts in the two bands. **a:** Light curves in 0.2-0.7 and 0.7-10 keV bands for XRF 050406. The bin size is 30 s for all but the last data point, which uses a 90 s bin. The count rates show that the rising part of the flare is significantly harder than the decaying part of the flare or the underlying afterglow. This strongly suggests that the flare is caused by a different emission mechanism than the rest of the afterglow. **b:** Light curves in 0.2-1.0 and 1-10 keV bands for GRB 050502B. The bin size is 10 s. The band ratio shows strong spectral variations during the large flare, with the ratio of counts in these bands decreasing by a factor of 4. The sharp spike in the hard band at about 740 s supports the internal shock interpretation for this flare, since such sharp features cannot easily be produced by external shocks.

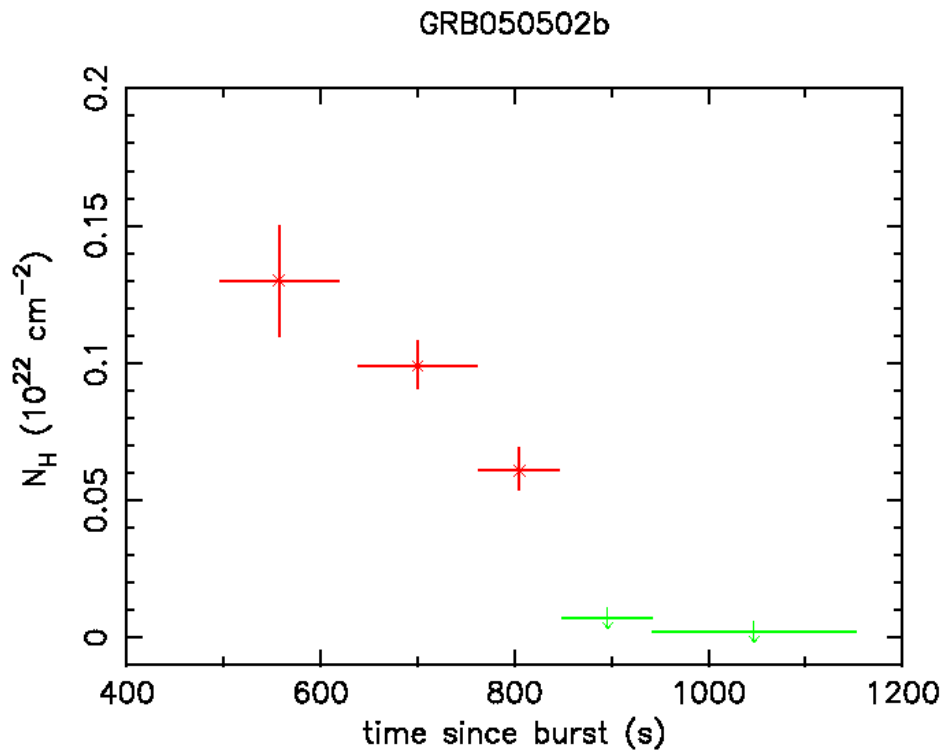


**Figure 3** Variations in intrinsic absorbing column density during the flare in GRB 050502B. The plot shows excess  $N_H$  (above the Galactic column, assuming  $z=0$ ) as a function of time. The absorbing column density drops substantially during the flare, suggesting that the absorbing gas is being photoionized during the X-ray flare. This puts strong constraints on the system geometry, as the absorbing gas must be relatively close to the ionizing object.

---

<sup>1</sup> Woosley, S. E. Gamma-ray Bursts from Stellar Mass Accretion Disks around Black Holes. *Astrophys. J.*, **405**, 273-277 (1993).

<sup>2</sup> Paczyński, B. Are Gamma-Ray Bursts in Star-Forming Regions? *Astrophys. J.*, **494**, L45-L48 (1998).

<sup>3</sup> MacFadyen, A. I., and Woosley, S. E., Collapsars: Gamma-Ray Bursts and Explosions in ``Failed Supernovae''. *Astrophys. J.*, **524**, 262-289 (1999).

<sup>4</sup> Mészáros, P., and Rees, M. J. Optical and Long-Wavelength Afterglow from Gamma-Ray Bursts. *Astrophys. J.*, **476**, 232-237

<sup>5</sup> van Paradijs, J., Kouveliotou, C., and Wijers, R. A. M. J. Gamma-Ray Burst Afterglows. *Ann. Rev. Astron. Astrophys.*, **38**, 379-425 (2000).

<sup>6</sup> Zhang, B., and Mészáros, P. Gamma-Ray Bursts: Progress, Problems, & Prospects. *Int. J. Mod. Phys.*, **19**, 2385-2472 (2004).

<sup>7</sup> Gehrels, N., et al. The Swift Gamma-Ray Burst Mission. *Astrophys. J.*, **611**, 1005-1020 (2004).

<sup>8</sup> Burrows, D. N. et al. The Swift X-ray Telescope. *Space Sci. Rev.*, in press (2005).

<sup>9</sup> Barthelmy, S. et al. The Swift Burst Alert Telescope. *Space Sci. Rev.*, in press (2005).

<sup>10</sup> Burrows, D. N., et al. Swift X-ray Telescope and Very Large Telescope Observations of the Afterglow of GRB 041223, *Astrophys. J.*, **622**, L85-L88 (2005).

<sup>11</sup> Campana, S., et al. Swift Observations of GRB 050128: the Early X-Ray Afterglow. *Astrophys. J.*, **625**, L23-L26 (2005).

<sup>12</sup> Tagliaferri, G., et al. The steeply decaying early afterglow of two Gamma Ray Bursts observed by Swift. *Nature*, submitted (2005).

<sup>13</sup> Cusumano, G., et al. Swift Observations of the Afterglow of GRB 050319. *Astrophys. J.*, submitted (2005).

<sup>14</sup> Piro, L., et al. Probing the Environment in Gamma-Ray Bursts: the Case of an X-ray Precursor, Afterglow Late Onset, and Wind Versus Constant Density Profile in GRB 011121 and GRTB 011211. *Astrophys. J.*, **623**, 314-324 (2005).

---

<sup>15</sup> Ioka, K. Kobayashi, S., and Zhang. B. Long-acting Engine or Strong Temporal Anisotropy Inferred from Variabilities of Gamma-ray Burst Afterglows. *Astrophys. J.*, submitted (2005).

<sup>16</sup> Kobayashi et al. Inverse Compton X-ray Flares from GRB Reverse Shock. *Astrophys. J.*, submitted (2005).

<sup>17</sup> Kobayashi et al. Can Internal Shocks Produce the Variability in Gamma-Ray Bursts? *Astrophys. J.*, **490**, 92-98 (1997).

<sup>18</sup> Zhang, B. & Mészáros, P. An Analysis of Gamma-Ray Burst Spectral Break Models. *Astrophys. J.*, **581**, 1236-1247 (2002).

<sup>19</sup> Waxman, E. & Draine, B. T. Dust Sublimation by Gamma-ray Bursts and Its Implications. *Astrophys. J.*, **537**, 796-802 (2000).

<sup>20</sup> Woods, E., and Loeb, A. Constraints on Off-Axis X-Ray Emission from Beamed Gamma-Ray Bursts. *Astrophys. J.*, **523**, 187-191 (1999).

<sup>21</sup> Zhang, B., Dai, X., Lloyd-Ronning, N. M., and Mészáros, P. Quasi-universal Gaussian Jets: A Unified Picture for Gamma-Ray Bursts and X-Ray Flashes. *Astrophys. J.*, **601**, L119-L122 (2004).

<sup>22</sup> MacFadyen, A. I., Woosley, S. E., and Heger, A. Supernovae, Jets, and Collapsars. *Astrophys. J.*, **550**, 410-425 (2001).

<sup>23</sup> Parsons, A., et al. Swift-BAT detection of GRB 050406. *GCN Circular* **3180** (2005).

<sup>24</sup> Krimm, H., et al. GRB 050406 BAT refined analysis. *GCN Circular* **3183** (2005).

<sup>25</sup> Falcone, A., et al. Swift Detection of the Bright Burst GRB050502b. *GCN Circular* **3330** (2005).

<sup>26</sup> Cummings, J., et al. GRB050502b Swift-BAT refined analysis. *GCN Circular* **3339** (2005).

<sup>27</sup> Heise, J. et al. X-ray Flashes and X-ray Rich Gamma-Ray Bursts, in *Gamma-Ray Bursts in the Afterglow Era* (eds Costa, E., Frontera, F., & Hjorth, J.) (Berlin Heidelberg: Springer, p. 16, 2001).

<sup>28</sup> Hill, J.E., et al. Readout Modes and automated operation of the Swift X-Ray telescope. *Proc. SPIE*, **5165**, 217-231 (2004).